International Journal of Applied Pharmaceutics

ISSN- 0975-7058 Vol 16, Issue 5, 2024

Original Article

COMPUTATIONAL ASSESSMENT OF *UNDARIA PINNATIFIDA* AND *MORINGA OLEIFERA* COMPOUNDS AS ANTI-OBESITY AGENTS

C. SAI KALYANI YOGINI[1], CHITTA SURESH KUMAR[2], C. M. ANURADHA[3], C. H. M. KUMARI CHITTURI[*]

[1]Department of Bio Medical Sciences, Assistant Professor, School of Health Sciences, the Apollo University, Chittoor-517127, Andhra Pradesh, India. [2,3]Department of Biochemistry, Srikrishnadevaraya University, Ananthapuram-515003, India. [*]Department of Applied Microbiology and Biochemistry, Sri Padmavati Mahila Vishvavidyalayam, (Women's University), Tirupati, Andhra Pradesh, India

[*]Corresponding author: C. H. M. Kumari Chitturi; [*]Email: chandi2222002@yahoo.co.in

Received: 15 Mar 2024, Revised and Accepted: 29 Jun 2024

ABSTRACT

Objective: The objective of this topic is to discuss the potential of using bioactive substances of *Undaria Pinnatifida* Ethanolic Extract of (UPEE) and *Moringa Oleifera* Methanolic Extract of (MOME) extracts as pharmacological agents and inhibitors of Peroxisome Proliferator-Activated Receptor gamma (PPAR-γ), Fat Mass and Obesity-Associated (FTO), Resistin and leptin to counter obesity.

Methods: The study uses Gas Chromatography-Mass Spectrometry (GC-MS) and Fourier-Transform InfraRed (FTIR) Spectroscopy techniques to identify the bioactive components of these extracts and evaluates their efficacy through in silico assessments and molecular docking analysis.

Results: Analysis of docking results revealed that ligand interaction with FTO (ID: 3LFM) docking complex showed good binding affinity, binding oreintation, pharmocological properties. Hence, the best ligands were proposed as the best antagonist to block PPAR-γ, FTO, Resistin and leptin, which plays major role in the drug devolopment pathways.

Conclusion: UPEE and MOME extracts acts as pharmacological agents for anti-obesity genes. PPAR-γ-4CI5 has a best docking score (-7.716 kcal/mol), as a result. As a result, the standard was recommended as the best antagonist to block the key enzyme involved in the drug development pathways.

Keywords: Obesity, *Undaria pinnatifida, Moringa oleifera,* PPAR γ, Molecular docking

DOI: https://dx.doi.org/10.22159/ijap.2024v16i5.50867 Journal homepage: https://innovareacademics.in/journals/index.php/ijap

INTRODUCTION

Obesity, characterized by excess fat accumulation, affects about half of the global population, as reported by the World Health Organization (WHO) in 2016 [1]. Contributing factors include genetic predisposition, energy imbalance, and excessive calorie intake [2]. It is associated with various degenerative diseases such as type 2 diabetes, cardiovascular conditions, and certain cancers [3]. The primary approach to combat obesity involves medications like orlistat, which inhibit pancreatic lipase expression, leading to delayed fat breakdown and subsequent loss through faeces [4, 5]. However, some anti-obesity medications have had limitations due to side effects [6, 7]. Fucoxanthin, a unique allenic carotenoid, has shown promise in inhibiting lipogenic enzyme activities and improving insulin sensitivity [8]. Natural substances like *Undaria pinnatifida* contain bioactive compounds with antioxidant, antitumor, anti-hypertensive, hypolipidemic, and immunoregulatory properties [9, 10]. Scientific literature has extensively demonstrated the beneficial effects of *Moringa oleifera*, a nutritious herb and miracle tree. It has been shown to improve lipid profiles, reduce body weight, enhance insulin signalling, and regulate satiety hormones like ghrelin and leptin [11]. *Moringa oleifera* is rich in various nutrients, including carbohydrates, amino acids, minerals like potassium and calcium, vitamins, oils, isothiocyanates, and phenolics such as Rutin, p-Coumaric acid, Chlorogenic acid, Kaempferol, and Quercetin [12, 13]. Moreover, it possesses therapeutic properties, including anticancer, antioxidant, anti-obesity, anti-ulcer, antiepileptic, antipyretic, and anti-inflammatory effects [14].

In the field of bioactive medication interactions, kinetic assessments and in silico molecular docking analyses are commonly employed techniques [15-17]. Additionally, in silico analytical methods like semi-empirical quantum mechanics and cheminformatics tools such as pre-Absorption, Distribution, Metabolism, Excretion, and Toxicity (ADMET) properties can accurately predict chemical properties and drug-like behaviour, aiding in drug development processes [18].

MATERIALS AND METHODS

FTIR analysis

One of the most useful instruments for identifying the many kinds of chemical bonds (also known as functional groups) that are present in compounds is the FTIR, following standard procedure [34]. The wavelength of light absorbed indicates the nature of the chemical bond, as can be seen in the annotated spectrum. Dried powders of different solvent extracts of every plant material were employed for FTIR analysis. 100 mg of Potassium Bromide (KBr) pellet and 10 mg of dried extract powder were combined to create translucent sample discs. FTIR was filled with a powdered sample of each plant specimen.

GC-MS analysis

The process of extracting UPEE and MOME was taken Department of Science and Technology (DST) Consolidation of University Research for Innovation and Excellence (CURIE) Sri Padmavathi Mahila Vishwa Vidyalayam (SPMVV) (Women's University), Tirupati, a standard GC-MS model to analyse a whole plant extract (methanolic) [19, 35]. The Agilent 7890 GC-MS apparatus and Flame Ionisation Detector (FID) detector were used and ran for 35 min in total. The instrument used was the Joel Accu Time of Flight (TOF) Analyzer for Mass Spectroscopy (MS). The resolution is 6000 and the mass range is 10-2000 amu. Splitless injection (20:80-8-200-5M-8-260-10M-10-280-HP5-ETOH) of 1.0 l of the sample in methanol was used for GC-MS analysis. The gas chromatograph, a Hewlett Packard 6890 Unites States of America (USA), was fitted with a cross-linked 5 percent phenyl methyl Siloxane Hewlett Packard (5%-phenyl)-methylpolysiloxanephasecapillary column (length 30 mm x internal diameter 0).

GC-MS operating conditions

The initial column temperature was 35 °C, with a 3-minute hold time. The temperature was set to rise at an 8 °C/min rate, with a final temperature of 280 °C. 1l of the sample was injected into the

port, vaporized, and moved down the column with helium as the carrier gas at a flow rate of 1 ml/min. At 70 eV, the MS Spectrum was captured. Following the separation in the column, the components were identified and analysed further using the FID. The compounds were identified by comparing the spectrum of unknown compounds to the spectrum of known compounds in the National Institute of Standards and Technology (NIST) mass spectral 2.0 structural library to determine their names, molecular weight, and structure.

In silico analysis of anti-obesity proteins

Retrieval and visualization of structure of anti-obesity proteins (PPAR-γ, α-Glucosidase, FTO, Resistin, Leptin)

The 3-dimensional atomic coordinates of a protein determine its tertiary structure [18]. Proteins can perform a variety of tasks, from molecular recognition to catalysis, and these tasks call for a precise tertiary structure. The primary structure of the biomolecules, or the order of the amino acids, is important for determining tertiary structure. Databases for protein tertiary structures such Protein Data Bank (PDB) sum, PDB and Molecular Modelling Database (MMDB), etc. The PDB sum provides a summary of all macromolecular structures that have been stored in the PDB, together with schematic diagrams of the molecules that make up each structure and their relationships. Other domains include links to literature, similar sequences, information about compounds bound to structure, and other domains are also included.

The 3-dimensional structural information of big biological molecules like proteins and nucleic acids is stored in the PDB. Global biochemists and biologists contribute the data, which is commonly obtained using X-ray crystallography or Nuclear Magnetic Resonance (NMR) spectroscopy. The data are available online. PDB is the most important source for structural biology information. About 15% of the structures were established using protein NMR while a small number were even determined by cryo-electron microscopy. X-ray diffraction is used to determine many structures. The protein structure's 3-dimensional coordinate file can be downloaded from PDB and viewed using programmes like PyMOL, Rasmol, Cn3 dimensional, Swiss protein database viewer, and molscript, among others.

The crystal structures of PPAR-γ (ID: 4CI5), α-Glucosidase (7P2Z) FTO (ID: 3LFM), Resistin (1LV6), Leptin (ID: 1AX8), were acquired from the PDB and visualised using Maestro v13.0 both biological macromolecules like proteins and tiny molecules can be rendered in stunning 3-dimensional visuals.

Virtual screening

Screening is virtually the main application of docking software. A computational method called virtual screening is used to explore databases of small molecules for those structures that are most likely to be therapeutic targets for protein receptors or enzymes [20, 21]. Virtual screening often comes in two Flavors: docking, or screening based on structure, and ligand-based virtual screening, or screening based on active compounds as templates. A technique called protein-ligand docking sometimes referred to as structure-based virtual screening, and involves comparing ligands to protein targets and then using a scoring function to ascertain whether the ligand will bind to the protein with a high affinity [22].

Virtual screening is a complementary method to experimental Standard Precision (SP) that analyses enormous databases of chemical compounds using computers to identify potential drug candidates SP. As part of the process of developing novel drugs, SP technology enables the testing of hundreds to millions of molecules for activity against a new target system. One of the main goals of the drug discovery process is to identify novel chemical compounds that have a high probability of binding to the target protein and causing the intended biological effect. Structure-based virtual screening involves a number of phases.

Compiling ligand dataset

UPEE and MOME were analysed using GC-MS, and bioactive substances like fucoxanthin, fucosterol, and fucoidan were found. Octahydro-1H-1,3,2-benzodiazaphosphole, 2-(3-Methylphenoxy) 1,4,10,13,16-diazacyclooctadecane, and 2-oxide Benzaldehyde, Thiofene, D-Threonine, N, N'-Ethylenebis(N-nitroacetamide), Methoxyacetic anhydride acid and 13-Pentano-1,4,10-trioxa-7,13-diazacyclopentadecane have significant therapeutic potential. Consequently, the existence of these phytochemicals may be to blame for the plant's medicinal properties.

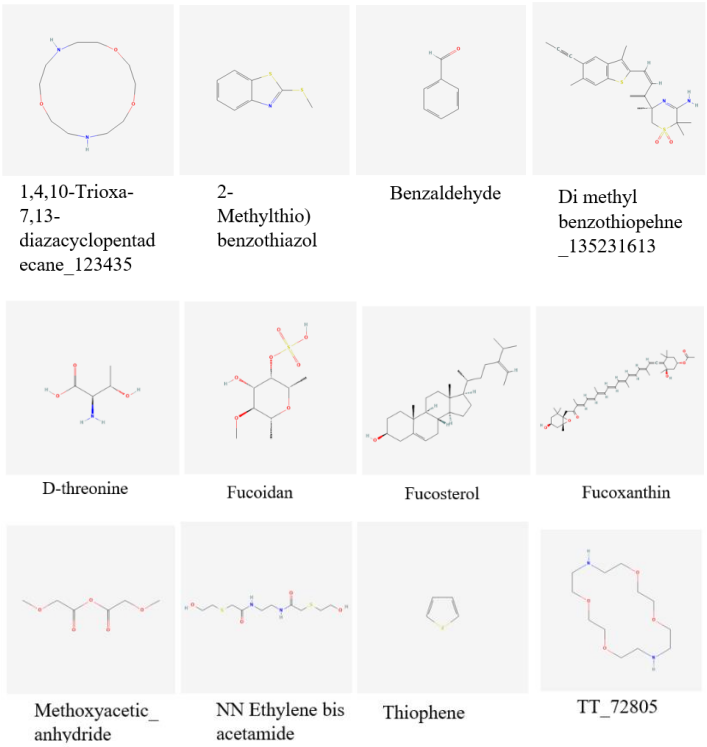

Fig. 1: Ligands retrieved from PubChem

The primary ligand sources for applications involving virtual screening are small molecule databases. To achieve the best results in computational docking research, the numerous chemicals present in small molecule databases must be simplified and optimised.

By incorporating tautomeric, stereochemical, and ionization variants, energy minimization, and customizable filters, LigPrep creates completely personalized ligand libraries by going much beyond straightforward 2-dimensional to 3-dimensional structural translations. That are suited for subsequent computational investigations. LigPrep can extend stereoisomers, ring conformations, tautomeric and ionisation states, and ionisation states to generate a wide range of chemical and structural diversity from a single input structure. Epik is a programme for generating the likely ionised and tautomerized structures within a specified pH range, as well as for predicting the pKa values of the ionizable groups in ligands.

Both physically important descriptors and qualities that are important for medicinal applications are predicted by the analogues UPEE and MOME. It includes primary descriptors, physiochemical characteristics, and a thorough examination of absorption. Drug design must consider distribution, metabolism, excision, and toxicity prediction. The UPEE and MOME principles for the last batch of promising leads against PPARG γ (ID: 4CI5), glucosidase (ID: 7P2Z), FTO (ID: 3LFM), resistin (ID: 1LV6), and leptin (ID: 1AX8).

Protein preparation

The three-dimensional arrangement of PPAR-γ or (ID: 4CI5), α-Glucosidase (ID: 7P2Z), FTO (ID: 3LFM), Resistin (ID: 1LV6), Leptin (ID: 1AX8), The Maestro (13) protein preparation procedure was used to pre-process adiponectin (ID: 4D04) (Schrodinger LLC, 2022). After adding all the hydrogens, the impact molecular mechanics engine and Optimised Potentials for Liquid Simulations (OPLS) 2005 force field were used to minimise the hydrogens (Schrodinger LLC, 2022). The heavy atoms were minimised by turning off the hydrogen torsion parameters, allowing the hydrogens to rotate freely. The maximum Root mean Square Deviation (RMSD) was set at 0.30Å.

Computational docking using Schrodinger software

A simulation method called "molecular docking" can be used to predict the shape of a complex between a tiny chemical and a protein receptor. It is also known as a simulation technique in which the location of a ligand in an anticipated or predetermined binding site of the receptor molecule is approximated.

The docking and scoring calculations were performed Glide v6.0, available in Schrodinger 2022. From the High-Throughput Virtual Screening (HTVS) mode, which effectively enriches millions of compound libraries, to the SP, which consistently docks tens to hundreds of thousands of ligands with high accuracy, to the Extra Precision (XP) mode, which further eliminates false positives through more extensive sampling and advanced scoring, leading to even higher enrichment, Glide offers the full range of speed vs. accuracy options. Glide approximates a comprehensive systematic search of the conformational, orientation, and positional space of the docked ligand.

For the constructed protein, a receptor grid was created so that different ligand configurations would bind within the anticipated binding region during docking. The grid in Glide was created using the OPLS 2005 force field with the default values of the van der Waals scaling factor of 1.00 and the charge cutoff of 0.25. The centroid of the binding site residues served as the centre of a cubic box that was created to a specified size. For the docking experiments, the bounding box was set to 10 Å x 10 Å x 10Å.

The ligand dataset (prepared ligands and published inhibitors) was docked into the grid of structure using Glide. Glide SP mode was applied for the prepared ligands along with published inhibitors in PPAR-γ (ID: 4CI5), α-Glucosidase (ID: 7P2Z), FTO (ID: 3LFM), Resistin (ID: 1LV6), Leptin (ID: 1AX8), Adiponectin (ID: 4D04). The lead molecules with least docking score were ranked and evaluated for ADMET properties using QikProp. The obtained docking score of leads were compared with existing inhibitors.

Orlistat with anti-obesity proteins

The anti-obesity proteins PPAR-γ (ID: 4CI5), α-Glucosidase (ID: 7K9N), FTO (ID: 3LFM), Resistin (ID: 1RFX), Leptin (ID: 3V6O) were aimed at molecular docking for virtual ligand screening with Orlistat.

RESULTS

FTIR analysis of *Undaria pinnatifida*

An analysis of algal biomass using Fourier infrared spectroscopy showed the presence of phenols, OH groups, phenols, carboxylic acids, halogens, methyl groups vinyl compounds, amides, alkenes and alkyl halide organic compound groups.

Table 1: Compounds from FTIR analysis of *U. Pinnatifida*

Peak values	Functional groups
3942.55-3687.45	O-H Stretching
3583.62	Phenols
3288.63	C-H
3251.23	carboxylic acid
2329.51	C-N
928.1	C=C alkene
500	halogens
421.33	Alkyl halides

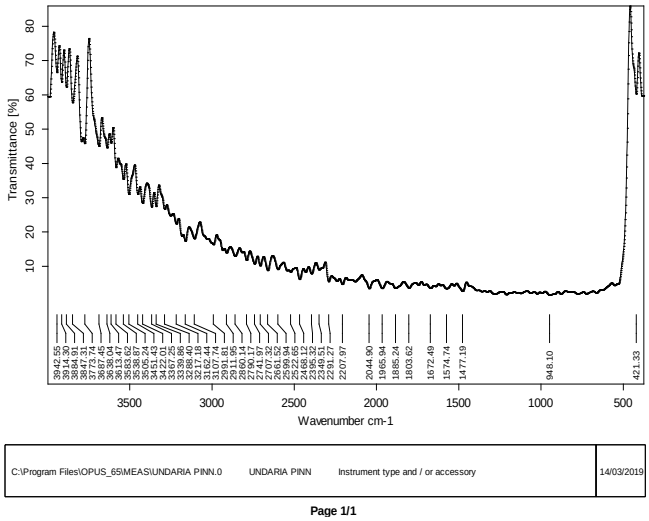

Fig. 2: FTIR analysis of UPEE

FTIR analysis of MOME

An analysis of algal biomass using Fourier infrared spectroscopy showed the presence of phenols, aldehyde alkanes, amines, methyl groups, vinyl compounds, amides, hydroxyl (OH) groups and carboxylic acids organic compound groups.

GC-MS analysis of *Undariapinnatifida*

Moringa oleifera leaves were subjected to phytochemical and GC-MS profiling, which indicated the presence of bioactive compounds such as fucoxanthin, pentaborane, D-Threonine, 13-Pentano-1,4,10-trioxa-7,13-diazacyclopentadecane, propanoic acid and hydroxypropanoic acid possessing significant therapeutic qualities. Therefore, the plant's medicinal properties may be due to the presence of these phytochemicals.

Table 2: Compounds from FTIR analysis of *Moringa oleifera*

Peak values	Functional groups
3634.77	O-H Stretching
3556.36	Phenols
3494.47	C-H stretching
3437.34	N-H
3309.13	carboxylic acid
1636.43	C=C alkene
516.35	halogens

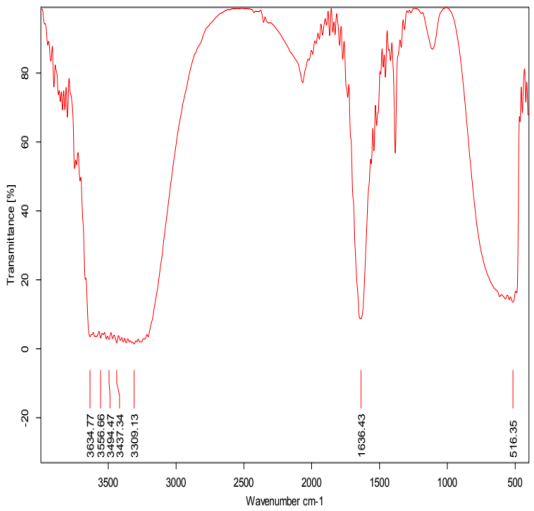

Fig. 3: FTIR analysis of MOME

Table 3: GC-MS analysis for bioactive components in UPEE

R. time	Area %	Compund name
0.066	81.09	2-(3-Methylphenoxy)octahydro-1H-1,3,2-benzodiazaphosphole 2-oxide
0.875	0.43	Hydrochloric Acid
1.24	0.27	Hexaborane
27.77	0.14	Benzaldehyde,
28.385	1.24	Fucoxanthin
28.678	1.67	Fucoidan
29.103	2.29	Fucosterol
1.363	0.13	benzene
1.058	0.7	1,3-Difluoro-2-propanol

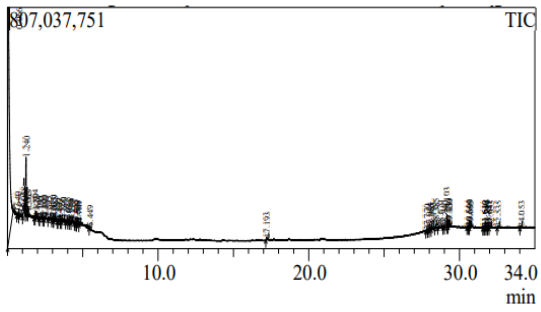

Fig. 4: GC-MS analysis of UPEE

GC-MS analysis of *Moringa oleifera*

The phytochemical compounds of MOME were identified based on mass spectra by comparing them with spectrum known components stored in NIST WILEY library. The active compounds in the extract of with their Retention Time (RT), area percentage were Pentaborane (1.112 retention time and 10.55% peak area), 4,7,13-Trioxa-1,10-diazacyclopentadecane (1.246 retention time and 82.37 % peak area), D-Threonine(1.511 retention time and 6.77% peak area), N, N'-Ethylenebis(N-nitro acetamide) (10.338 retention time and 0.13% peak area), Fucosterol (29.103 retention time and 2.29 % peak area) and Acetic acid, methoxy-, anhydride (10.82 retention time and 0.04 % peak area). Hence, the presence of these phytochemicals could be responsible for the therapeutic effects.

Table 4: Compounds from GC-MS analysis of *Moringa oleifera*

R. time	Area %	Compund name
1.112	10.55	Pentaborane (9)
1.246	82.37	4,7,13-Trioxa-1,10-diazacyclopentadecane
1.511	6.77	D-Threonine

10.338	0.13	N,N'-Ethylenebis(N-nitroacetamide)
29.103	2.29	Fucosterol
10.82	0.04	Acetic acid, methoxy-, anhydride

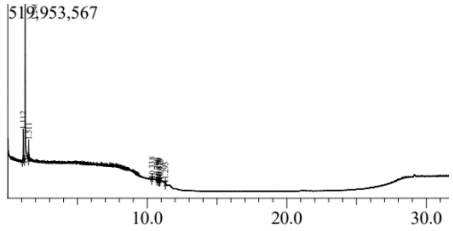

Fig. 5: GC-MS analysis of MOME

Fig. 6: *PPAR-γ* (ID: 4CI5)

In silico analysis of anti-obesity proteins

***PPAR-γ* (PDB ID: 4CI5)**

The co-crystal structure of PPAR-γ (ID: 4CI5) is retrieved and visualized by using the visualization tool PyMOL. The active site residues which are involved in bonding with ligand 2-methyl-2-[4-[2-[4-[(E)-phenyldiazenyl] phenoxy] ethyl]phenoxy]propanoic acid PDB site records.

Computational docking using schrodinger

A receptor grid of 10Å x 10Å x 10Å was generated around active site residues fun initial docking of 13 ligand molecules docked with significant docking score. The best lead fucosterol (lead-1) showed the lowest docking showed score of -6.709kcal/mol (figure).

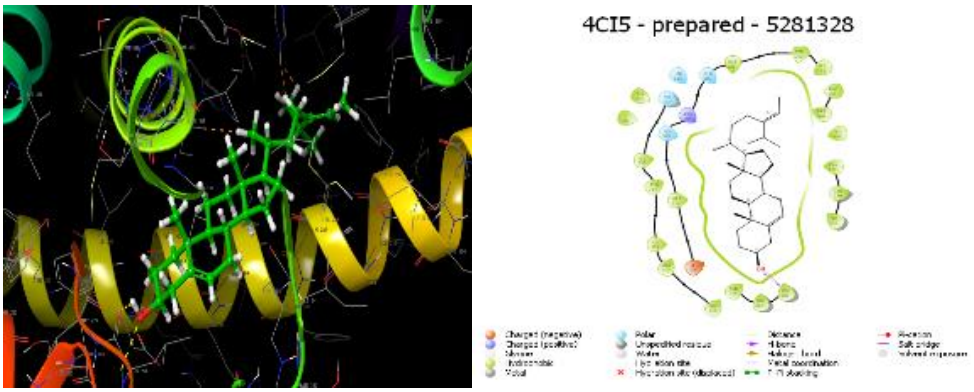

Fig. 7: Molecular interactions of PPAR-γ (PDB ID: 4CI5) with fucosterol (5281328)

Lcu 229 formed two hydeogen bonds with ligand. The active residues such as The active site residues such as His-121, Tyr-127, Glu-205, Lcu-229, Ser-289, Ser-299, Glu-295, Ser-299, His-323, Ilu-326, Icc-440, His-449, Tyr-473 formed in molecular interactions were also well correlated with the active site residues of native co-crystal structure of PPAR-γ (PDB ID: 4CI5) and the residues Phe-226, Pro-227, Ala-292, Tyr-327, Met-329, Leu-333, His-449, Leu-453, Tyr-473 were around the active site (within 4 A°) found to be present involed in van der Waals interactions with ligand.

Analysis of docking results revealed that ligand interaction (Aminocyclitol) with protein PPAR-γ docking complex showed good binding affinity, binding orientation, pharmocological properties. The formation of hydrogen bond along with the residues involed in van der Waals interctions were also highly important for the stability of the docking complex. Hence, lead-1with better docking score (6.709kcal/mol). Hence, the ligands were proposed as the best antagonist to block PPAR-γ of, which plays major role in drug development.

Table 5: H-bond donor and acceptor and rotatable bonds and docking score with *PPAR-γ* with ligands

S. No.	Title	Entry name	Donor HB	Accpt HB	glide rotatable bonds	docking score
1	5281328	Fucosterol	1	1.7	6	-6.709
2	1.3E+08	Fucoidan	2	9.1	4	-6.503
3	11989	Benzothiazole	0	1.5	1	-6.111
4	72805	TT7	2	9.8	0	-6.024
5	69435	Threonine	3	3.7	3	-5.895
6	123435	Trioxadiazacyclopentadecane	2	8.1	0	-5.813
7	240	Benzaldehyde	0	2	1	-5.751
8	1032	Propionic acid	1	2	1	-5.269
9	8030	Thiofene	0	0	0	-4.521
10	88095	Methoxyacetic_anhydride	0	7.9	6	-3.697
11	1.02E+08	Ethylenebisacetamide	4	9.4	15	-2.219

*Hydrogen bond donor (<5), *Hydrogen bond acceptor (<10), *Number of rotatable bonds, *Docking score.

Table 6: ADMET properties as verified by using QikProp (Schrodinger 13) of *PPAR-γ* with ligands

S. No.	Title	Entry name	Mol MW	QPlog Po/w	QPlog S	QPP Caco	QPlog BB	QPP MDCK	QPlog Kp	QPlog Khsa	Percent Human oral absorption	Rule of five	Rule of three
1	5281328	Fucosterol	412.698	7.522	-8.722	3405.278	-0.292	1860.133	-1.718	2.071	100	1	1
2	1.3E+08	Fucoidan	256.27	-0.047	-1.192	100.862	-0.959	53.808	-3.752	-1.126	62.533	0	0
3	11989	Benzothioazole	181.27	3.031	-2.735	6656.771	0.574	10000	-1.097	-0.074	100	0	0
4	72805	TT7	262.348	0.099	2	402.712	0.098	226.545	-4.275	-1.265	74.148	0	0
5	69435	Threonine	119.12	-3.351	0.054	10.81	-0.639	5.218	-6.624	-1.026	25.826	0	1
6	123435	Trioxadiaza cyclopentadecane	218.295	-0.235	-0.015	286.124	1.068	156.57	-6.292	-0.528	69.536	0	0
7	240	Benzaldehyde	106.124	1.479	-1.116	1830.242	-0.08	950.803	-2.121	-0.657	94	0	0
8	1032	Proionicacid	74.079	0.606	0.284	239.776	-0.284	134.41	-3.405	-0.962	73.087	0	0
9	8030	Thiofene	84.136	1.815	-1.449	9906.038	0.192	10000	-0.841	-0.374	100	0	0
10	88095	Methoxyacetic _anhydride	162.142	-1.384	1.316	1124.064	-0.516	561.37	-2.972	-1.949	73.443	0	0
11	1.02E+08	Ethylenebis acetamide	296.399	-1.022	-0.349	30.277	-2.246	103.075	-4.17	-1.585	47.473	0	0

*Molecular weight (<500 Da), *Predicted octanol/water partition-efficient log P (acceptable range-2-6.5), *Predicted aqueous solubility test: S Mol/l(acceptable range6.5-0.5), *Apparent $Caco_2$ permeability nm/sec(<25 poor and>500 high), *prediction of brain/blood; (acceptable range-3.0-1.2),*Predicted apparent MDCK cell permeability in nm/s (<25 poor and>500 high),*log Kp for skin permeability (Kp in cm/hr), *log Khsa serum protein binding (-1.5-1.5), Lipinski rule of five violation (max is 4), Jorgenson rule of 3 violation (max is 3), *Percentage of Human oral absorption(<25%is poor and>80% is high), ADMET PROPERTIES: absorption, distribution, metabolism, excretion, toxicity.

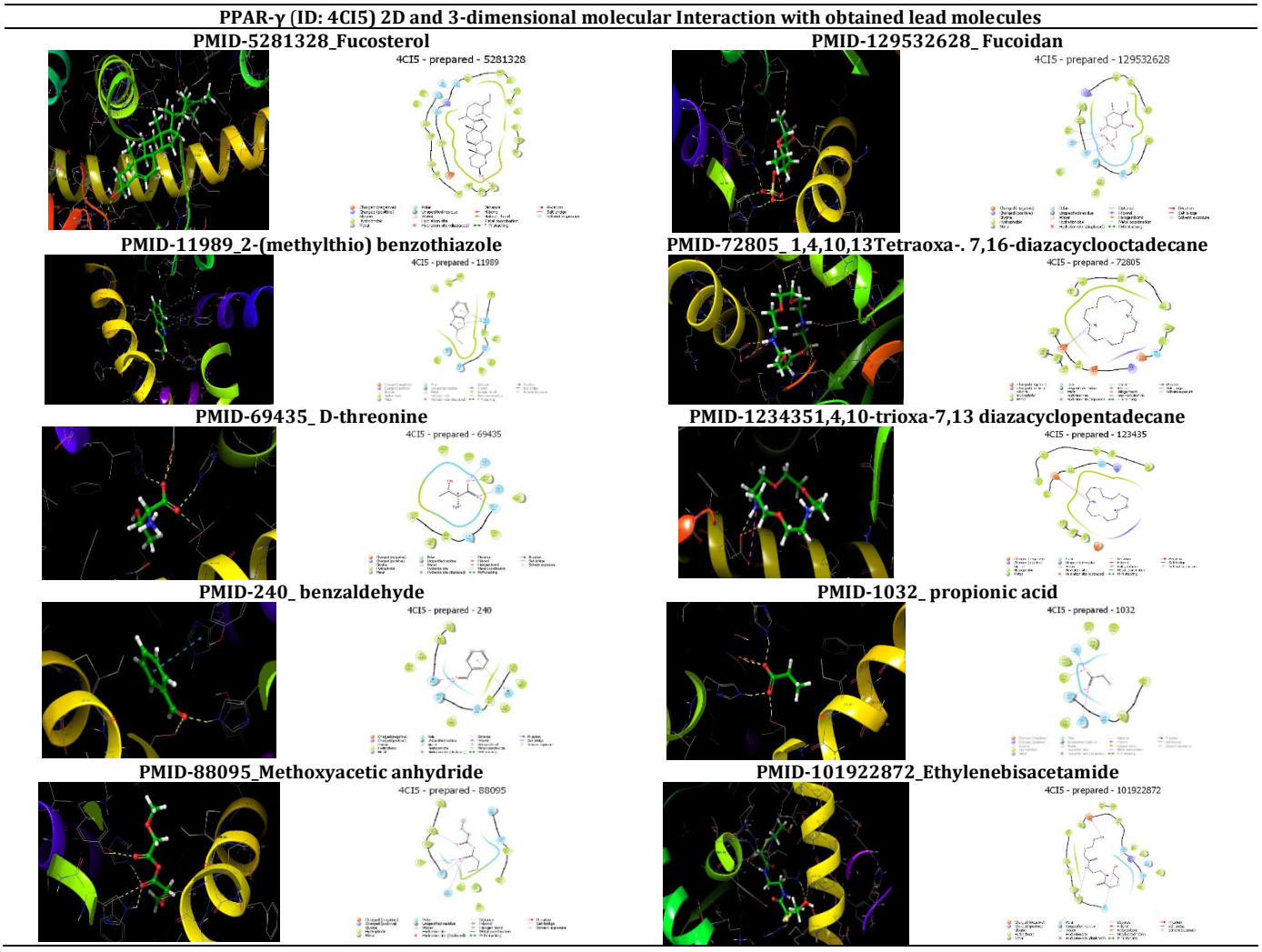

Fig. 8: Molecular interactions of PPAR-γ (PDB ID: 4CI5) with ligands

Alpha glucosidase (AG) (PDB ID: 7K9N)

The co-crystal structure of AG (ID: 7K9N) and visualized by using the visualization tool PyMOL. The active site residues which are involved in bonding with ligand W9G (Hydroxy Methyl methoxynonyl amino cyclohexane-tetrol) from the PDB site records.

Computational docking using schrodinger

A receptor grid of 10Å x 10Å x 10Å was generated around active site residues AG. Initial docking of 13 ligand molecules catalase docked with significant docking score. The best lead, Trioxadiazacyclopentadecane showed the lowest docking showed score of-6.466kcal/mol (fig).

ASP-640 created one salt bridge and one hydrogen bond, interaction with ligand. The active site residues such as Asp-34, Asp-305, Trp-423, Asp-451, Trp-525, Asp-564, Phe-571, Arg-624, Asp-640, Phe-673, Phe-674, His-698, His-700 formed molecular interactions were also well correlated with the active site residues of native co-crystal structure of AG and the residues Phe-307, Tyr-318, Trp-423, Ile-452, Ile-488, Trp-525, Trp-562, Met-565, Ser-569, Asn-572, Bal-576, Trp-637 were around the active site (within 4 A°) found to be present involed in van der Waals interactions with ligand.

Analysis of docking results revealed that ligand interaction with protein AG docking complex showed good binding affinity, binding orientation, pharmocological properties. The formation of hydrogen bonds along with the residues involved in van der Waals interactions were also highly important for the stability of the docking complex. Hence, lead-1 with a better docking score (-6.466kcal/mol). Hence, the best ligands are the best antagonist to block AG of antagonistsplays a major role in drug development.

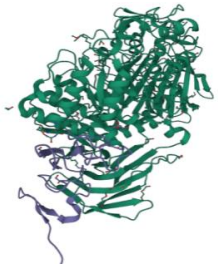

Fig. 9: AG (ID: 7K9N)

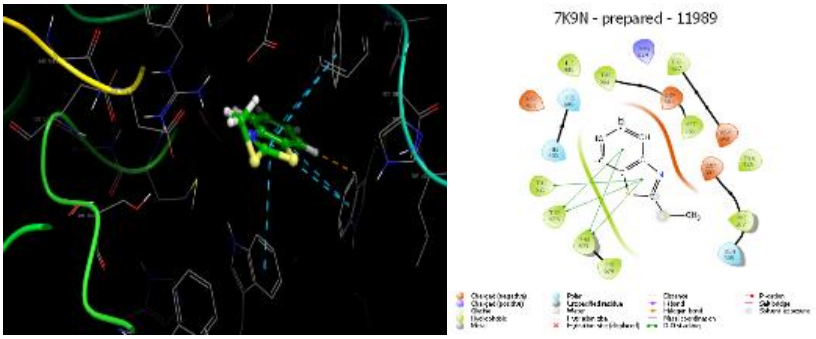

Fig. 10: Molecular interactions of AG (PDB ID: 7K9N)

Table 7: H-bond donor and acceptor and rotatable bonds and docking score with AG with ligands

Title	Entry name	Donor HB	Accpt HB	Glide rotatable bonds	Docking score
123435	Trioxadiazacyclopentadecane	2	8.1	0	-6.466
69435	Threonine	3	3.7	3	-5.736
240	Benzaldehyde	0	2	1	-5.308
72805	TT7	2	9.8	0	-5.229
11989	Benzothioazole	0	1.5	1	-5.103
5281328	Fucosterol	1	1.7	6	-4.496
8030	Thiofene	0	0	0	-4.244
1.3E+08	Fucoidan	2	9.1	4	-3.667
1.02E+08	Ethylenebisacetamide	4	9.4	15	-2.888
88095	Methoxyacetic_anhydride	0	7.9	6	-2.344
1032	Proionicacid	1	2	1	-1.322

*Hydrogen bond donor (<5), *Hydrogen bond acceptor (<10), *Number of rotatable bonds, *Docking score.

Table 8: ADMET properties of AG with ligands

S. No.	Title	Entry name	mol MW	QPlog Po/w	QPlog S	QPP Caco	QPlog BB	QPP MDCK	QPlog Kp	QPlog Khsa	Percent human oral absorption	Rule of five	Rule of three
1	123435	Trioxadiazacyclo pentadecane	218.295	-0.235	-0.015	286.124	1.068	156.57	-6.292	-0.528	69.536	0	0
2	69435	Threonine	119.12	-3.351	0.054	10.81	-0.639	5.218	-6.624	-1.026	25.826	0	1
3	240	Benzaldehyde	106.124	1.479	-1.116	1830.242	-0.08	950.803	-2.121	-0.657	94	0	0
4	72805	TT7	262.348	0.099	2	402.712	0.098	226.545	-4.275	-1.265	74.148	0	0
5	11989	Benzothioazole	181.27	3.031	-2.735	6656.771	0.574	10000	-1.097	-0.074	100	0	0
6	5281328	Fucosterol	412.698	7.522	-8.722	3405.278	-0.292	1860.133	-1.718	2.071	100	1	1
7	8030	Thiofene	84.136	1.815	-1.449	9906.038	0.192	10000	-0.841	-0.374	100	0	0
8	1.3E+08	Fucoidan	256.27	-0.047	-1.192	100.862	-0.959	53.808	-3.752	-1.126	62.533	0	0
9	1.02E+08	Ethylenebis acetamide	296.399	-1.022	-0.349	30.277	-2.246	103.075	-4.17	-1.585	47.473	0	0
10	88095	Methoxyacetic_ anhydride	162.142	-1.384	1.316	1124.064	-0.516	561.37	-2.972	-1.949	73.443	0	0
11	1032	Proionicacid	74.079	0.606	0.284	239.776	-0.284	134.41	-3.405	-0.962	73.087	0	0

*Molecular weight (<500 Da), *Predicted octanol/water partition-efficient log P (acceptable range-2-6.5), *Predicted aqueous solubility test: S Mol/l(acceptable range6.5-0.5), *Apparent $Caco_2$ permeability nm/sec(<25 poor and>500 high), *prediction of brain/blood; (acceptable range-3.0-1.2),*Predicted apparent MDCK cell permeability in nm/s (<25 poor and>500 high),*log Kp for skin permeability (Kp in cm/hr), *log Khsa serum protein binding (-1.5-1.5), Lipinski rule of five violation (max is 4), Jorgenson rule of 3 violation (max is 3), *Percentage of Human oral absorption(<25%is poor and>80% is high), ADMET properties.

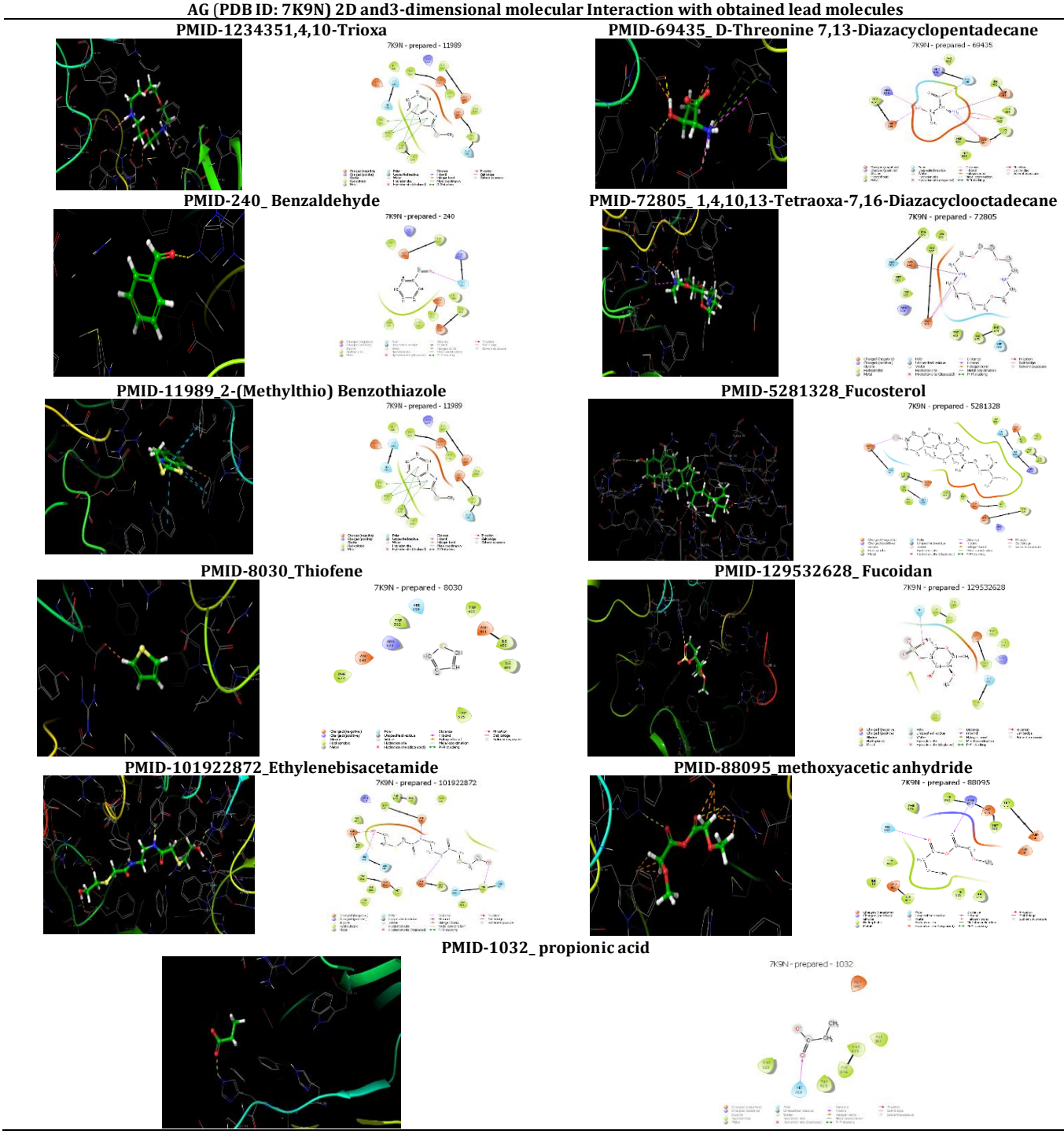

Fig. 11: Molecular interactions of AG (PDB ID: 7K9N) with ligands

FTO (ID: 3LFM)

The co-crystal structure of FTO (ID: 3LFM) and visualized by using the visualization tool PyMOL. The active site residues which are involved in bonding with ligand 3Metyl thymidine from PDB site records.

Computational docking using schrodinger

A receptor grid of 10Å x 10Å x 10Å was generated around active site residues FTO (ID: 3LFM). Initial docking of 13 ligand molecules catalase docked with significant docking score. The best lead (Benzothioazole) showed lowest docking showed score of-5.566kcal/mol (Figure).

Fig. 12: FTO (ID: 3LFM)

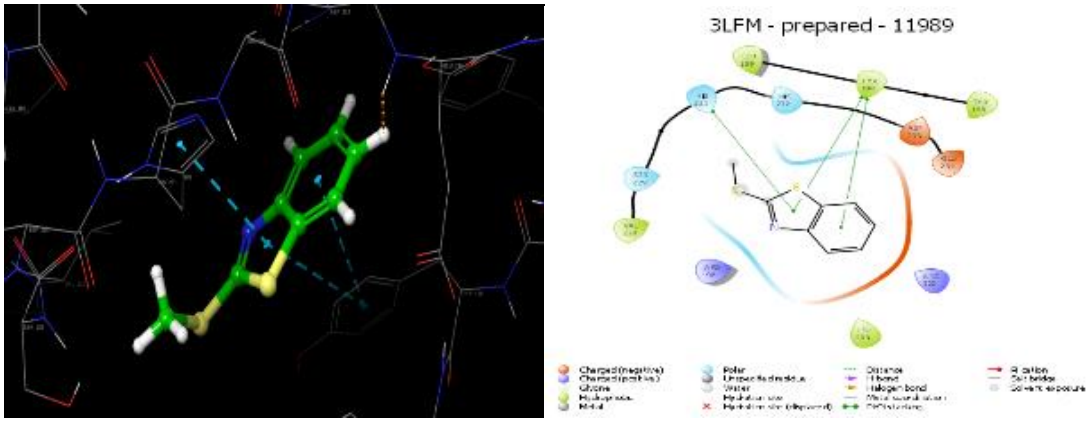

Fig. 13: Molecular interactions of FTO (ID: 3LFM)

Arg-108 Tyr-108 formed one hydrogen bond ASP-152 formed Pi-Pi staking interaction with ligand. Residues from the active site, includingArg-96, Tyr-108, Asn-205, Ser-229, His-231, His-232, Glu-234, Arg-322 formed in molecular interactions were also well correlated with the residuals from the active sites of native co-crystal FTO and the residues Ile-85, Leu90, Leu-91, Thr-92, Pro-93, Val94, Leu109, Met-212, Leu-215, Lys-216, Met-226, Ala-227, Val-228 were around the active site (within 4 A°) found to be present involed in van der Waals interactions with ligand.

Analysis of docking results revealed that ligand interaction with FTO (ID: 3LFM) docking complex showed good binding affinity, binding orientation, pharmocological properties. The formation of hydrogen bond along with the residues involved in van der Waals interactions were also highly important for the stability of the docking complex. Hence, lead-1 with better docking score (-5.566kcal/mol). Hence, the best ligands were proposed as the best antagonist to block FTO, which plays major role in the drug development pathways.

Resistin (ID: 1RFX)

The co-crystal structure of Resistin (ID: 1RFX) and visualized by using the visualization tool PyMOL. The active site residues which are involved in bonding with ligand Polyethylene glycol (Di Hydro ethyl) ether) from the PDB site records.

Table 9: H-bond donor and acceptor and rotatable bonds and docking score with FTO with ligands

S. No.	Title ID	Title	Donor HB	Accpt HB	glide rotatable bonds	docking score
1	11989	Benzothioazole	0	1.5	1	-5.566
2	240	Benzaldehyde	0	2	1	-5.164
3	123435	Trioxadiazacyclopentadecane	2	8.1	0	-5.115
4	72805	TT	2	9.8	0	-4.926
5	8030	Thiofene	0	0	0	-4.155
6	1.3E+08	Fucoidan	2	9.1	4	-4.095
7	5281328	Fucosterol	1	1.7	6	-3.734
8	69435	Threonine	3	3.7	3	-3.191
9	1032	Proionicacid	1	2	1	-3.092
10	88095	Methoxyacetic_anhydride	0	7.9	6	-3.082
11	1.02E+08	Ethylenebisacetamide	4	9.4	15	-0.876

*Hydrogen bond donor (<5), *Hydrogen bond acceptor (<10), *Number of rotatable bonds, *Docking score.

Table 10: ADMET properties of Fat mass and obesity-associated (FTO) with Ligands

S. No.	Title ID	mol. MW	Q Plog Pw	Q Plog S	Q Plog BB	QPP MDCK	Q Plog Kp	Q Plog khsa	Q Plog khsa	Rule of five	Rule of three
1	11989	181.27	3.331	-2.735	0.574	10000	-1.097	-0.074	-0.074	0	0
2	240	106.124	4.126	-1.116	-0.08	950.803	-2.121	-0.657	-0.657	0	0
3	123435	218.295	11.986	-0.015	1.068	156.57	-6.292	-0.528	-0.528	0	0
4	72805	262.348	9.787	2	0.098	226.545	-4.275	-1.265	-1.265	0	0
5	8030	84.136	1.647	-1.449	0.192	10000	-0.841	-0.374	-0.374	0	0
6	1.3E+08	256.27	12.586	-1.192	-0.959	53.808	-3.752	-1.126	-1.126	0	0
7	5281328	412.698	3.96	-8.722	-0.292	1860.133	-1.718	2.071	2.071	1	1
8	69435	119.12	8.848	0.054	-0.639	5.218	-6.624	-1.026	-1.026	0	1
9	1032	74.079	4.261	0.284	-0.284	134.41	-3.405	-0.962	-0.962	0	0
10	88095	162.142	8.217	1.316	-0.516	561.37	-2.972	-1.949	-1.949	0	0
11	1.02E+08	296.399	19.619	-0.349	-2.246	103.075	-4.17	-1.585	-1.585	0	0

*Molecular weight (<500 Da), *Predicted octanol/water partition-efficient log P (acceptable range-2-6.5), *Predicted aqueous solubility test: S Mol/l(acceptable range6.5-0.5), *Apparent $Caco_2$ permeability nm/sec(<25 poor and>500 high), *prediction of brain/blood; (acceptable range-3.0-1.2),*Predicted apparent MDCK cell permeability in nm/s (<25 poor and>500 high),*log Kp for skin permeability (Kp in cm/hr), *log Khsa serum protein binding (-1.5-1.5), Lipinski rule of five violation (max is 4), Jorgenson rule of 3 violation (max is 3), *Percentage of Human oral absorption (<25% is poor and >80% is high), ADMET PROPERTIEST: absorption, distribution, metabolism, excretion, toxicity.

FTO (ID: 3LFM) 2D and 3-dimensional molecular interaction with obtained lead molecules

PMID-11989_2-(Methylthio) Benzothiazole

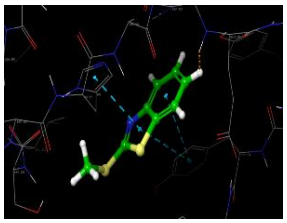

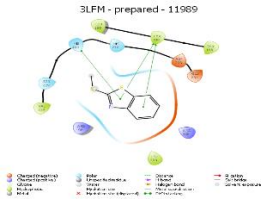

PMID-240_ Benzaldehyde

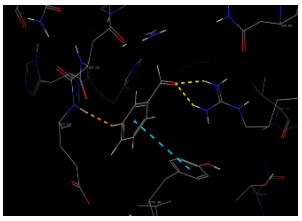

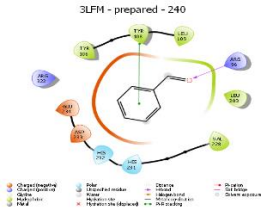

PMID-123435_ 1,4,10-Trioxa-Diazacyclooctadecane

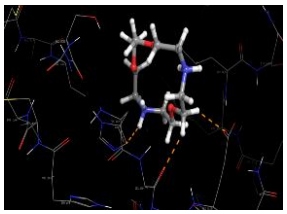

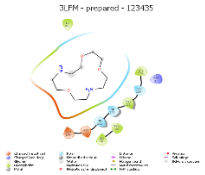

PMID-72805 7,167,13-Diazacyclopentadecane

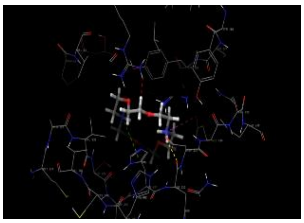

PMID-8030_Thiofene

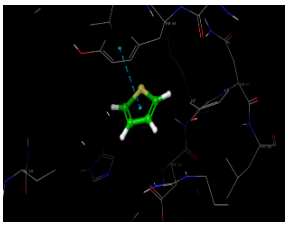

PMID-129532628_ Fucoidan

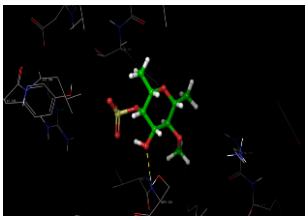

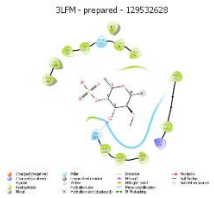

PMID-5281328_Fucosterol

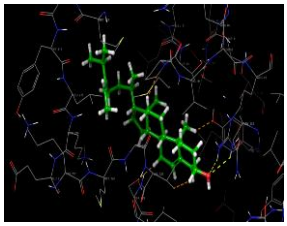

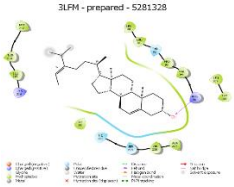

PMID-69435_ D-Threonine

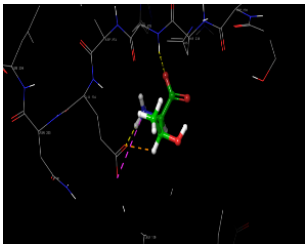

PMID-1032_ propionic acid

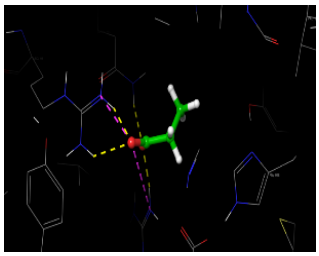

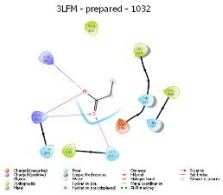

PMID-88095_methoxyacetic anhydride

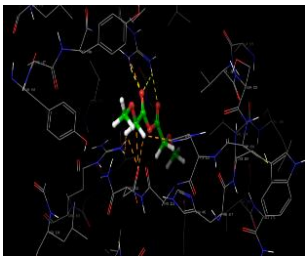

PMID-101922872_Ethylenebisacetamide

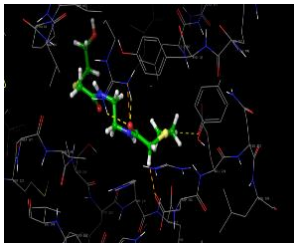

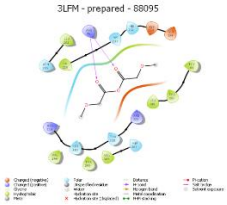

Fig. 14: Molecular interactions of fat mass and obesity associated (FTO) (PDB ID: 3LFM)

Fig. 15: Resistin (ID: 1RFX)

Computational docking using schrodinger

A receptor grid of 10Å x 10Å x 10Å was generated around the active site residues catalase. Initial docking of 13 ligand molecules catalase docked with significant docking score. The best lead (Benzothioazole) showed lowest docking showed score of -5.322kcal/mol (Figure).

Gln-C: 76 one hydrogen bond interaction with leading ligand. The active site residues such as Arg-B: 41, Trp-C: 65, Asp-C: 66, Ile-C: 67, Asp-B: 81, Trp-B: 82 formed in molecular interactions were also well correlated with the active site residues of native co-crystal structure of Resistin (ID: 1RFX) and the residues Trp-B: 36, Thr-B: 37, Ser-B: 39, Ser-B: 40, Arg-C: 68, Glu-C: 69, GlU-C: 70, Arg-b: 86 were around the active site (within 4 A°) found to be present involed in van der Waals interactions with ligand.

Analysis of docking results revealed that ligand interaction with Resistin (ID: 1RFX) docking complex showed good binding affinity, binding orientation, pharmocological properties. The formation of hydrogen bond along with the residues involved in van der Waals interactions were also highly important for the stability of the docking complex. Hence, lead-1 with better docking score (-5.322). Hence, the best ligands were proposed as the best antagonist to block Resistin (ID: 1RFX) of, which plays major role in the drug development pathways.

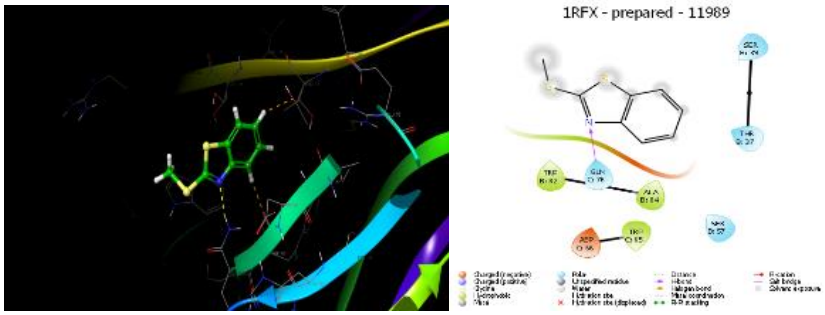

Fig. 16: Molecular interactions of resistin (ID: 1RFX)

Table 11: Docking score of Resistin (ID: 1RFX) with ligands

S. No.	Title ID	Title	Donor HB	Accpt HB	glide rotatable bonds	docking score
1	11989	Benzothiazole	0	1.5	1	-5.322
2	240	Benzaldehyde	0	2	1	-4.98
3	72805	TT	2	9.8	0	-4.601
4	123435	Trioxadiazacyclopentadecane	2	8.1	0	-4.393
5	8030	Thiofene	0	0	0	-4.346
6	1.3E+08	Fucoidan	2	9.1	4	-3.818
7	69435	Threonine	3	3.7	3	-3.485
8	88095	Methoxyacetic_anhydride	0	7.9	6	-3.339
9	1032	Proionicacid	1	2	1	-2.235
10	5281328	Fucosterol	1	1.7	6	-1.814
11	1.02E+08	Ethylenebisacetamide	4	9.4	15	-0.31

*Hydrogen bond donor (<5), *Hydrogen bond acceptor (<10), *Number of rotatable bonds, *Docking score.

Table 12: H-bond donor and acceptor and rotatable bonds and docking score with resist in (ID: 1RFX) with ligands

S. No	Title ID	mol MW	QPlog Po/w	QPlog S	QPP Caco	QPlog BB	QPP MDCK	QPlog Kp	QPlog Khsa	Percent Human oral absorption	Rule of five	Rule of three
1	11989	181.27	3.031	-2.735	6656.771	0.574	10000	-1.097	-0.074	100	0	0
2	240	106.124	1.479	-1.116	1830.242	-0.08	950.803	-2.121	-0.657	94	0	0
3	72805	262.348	0.099	2	402.712	0.098	226.545	-4.275	-1.265	74.148	0	0
4	123435	218.295	-0.235	-0.015	286.124	1.068	156.57	-6.292	-0.528	69.536	0	0
5	8030	84.136	1.815	-1.449	9906.038	0.192	10000	-0.841	-0.374	100	0	0
6	1.3E+08	256.27	-0.047	-1.192	100.862	-0.959	53.808	-3.752	-1.126	62.533	0	0
7	69435	119.12	-3.351	0.054	10.81	-0.639	5.218	-6.624	-1.026	25.826	0	1
8	88095	162.142	-1.384	1.316	1124.064	-0.516	561.37	-2.972	-1.949	73.443	0	0
9	1032	74.079	0.606	0.284	239.776	-0.284	134.41	-3.405	-0.962	73.087	0	0
10	5281328	412.698	7.522	-8.722	3405.278	-0.292	1860.133	-1.718	2.071	100	1	1
11	1.02E+08	296.399	-1.022	-0.349	30.277	-2.246	103.075	-4.17	-1.585	47.473	0	0

*Molecular weight (<500 Da), *Predicted octanol/water partition coefficient log P (acceptable range-2-6.5), *Predicted aqueous solubility test: S Mol/l(acceptable range6.5-0.5), *Apparent $Caco_2$ permeability nm/sec(<25 poor and>500 high), *prediction of brain/blood; (acceptable range-3.0-1.2),*Predicted apparent MDCK cell permeability in nm/s (<25 poor and>500 high),*log Kp for skin permeability (Kp in cm/hr), *log Khsa serum protein binding (-1.5-1.5), Lipinski rule of five violation (max is 4), Jorgenson rule of 3 violation (max is 3), *Percentage of Human oral absorption(<25%is poor and>80% is high), ADMET PROPERTIES: absorption, distribution, metabolism, excretion, toxicity.

Resist in (ID: 1RFX) 2D and3-dimensional molecular Interaction with obtained lead molecules

PMID-11989_2-(Methylthio) Benzothiazole

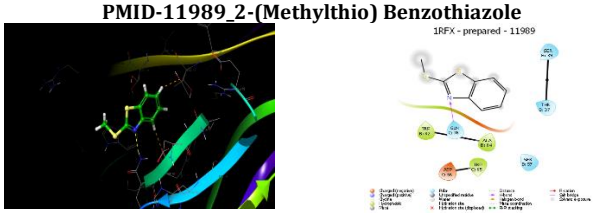

PMID-240_ Benzaldehyde

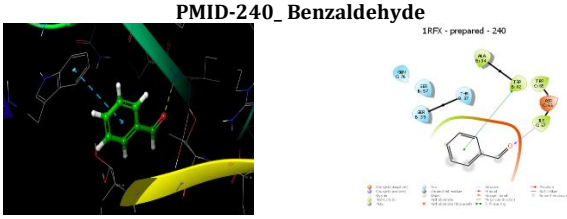

PMID-72805_ 1,4,10,13-7,13-Diazacyclopentadecane

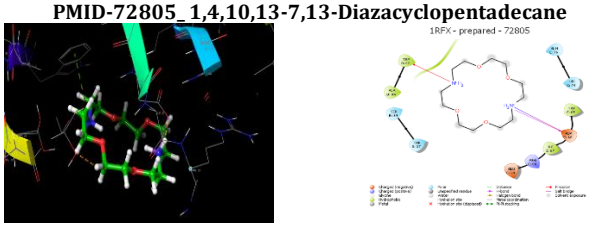

PMID-1234351,4,10-Trioxa Tetraoxa-7,16-Diazacyclooctadecane

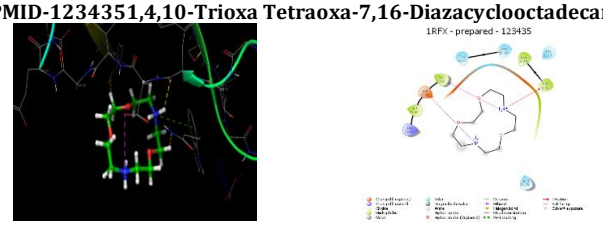

PMID-8030_Thiofene

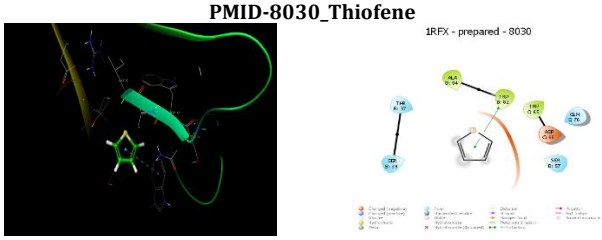

PMID-129532628_ Fucoidan

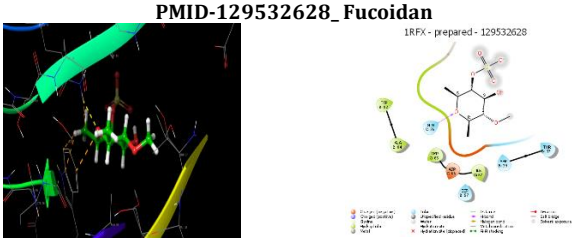

PMID-69435_ D-Threonine

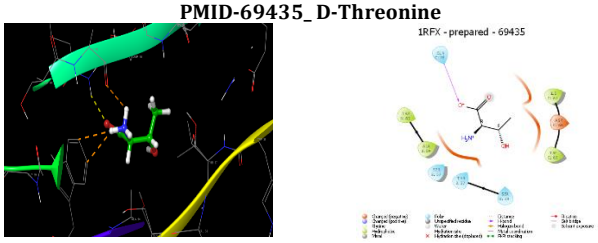

PMID-88095_Methoxyacetic anhydride

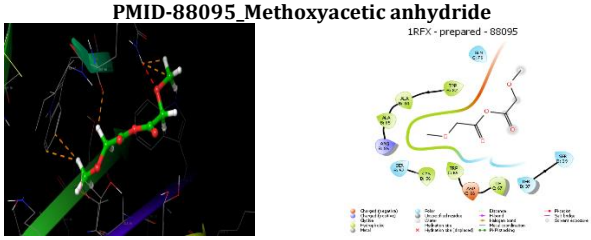

PMID-1032_ propionic acid

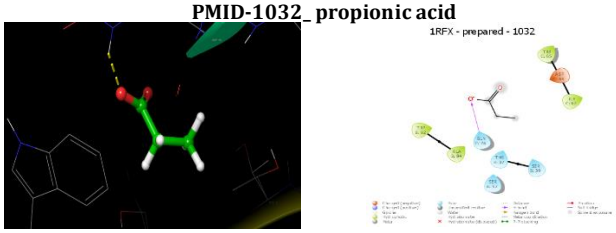

PMID-5281328_fucosterol

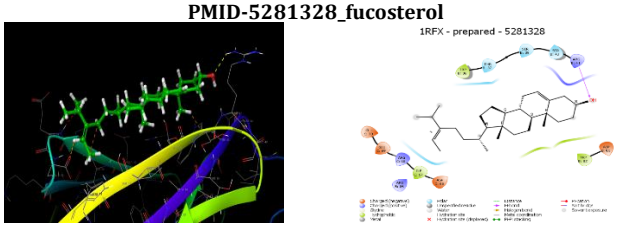

PMID-101922872_Ethylenebisacetamide

Fig. 17: Molecular interactions of resist in (ID: 1RFX) with ligands

Leptin (ID: 3V6O)

The co-crystal structure of Leptin (ID: 3V6O) and visualized by using the visualization tool PyMOL. The active site residues which are involved in bonding with ligand N acetylglucosamine (NAG) (2 cetamide-2-deoxy-beta-beta-D-Glycopyranose) from the protein database (PDB) site records.

Computational docking using schrodinger

A receptor grid of 10Å x 10Å x 10Å was generated around the active site residues catalase. Initial docking of 13 ligand molecules catalase docked with significant docking score. The best lead (2-(Methylthio) Benzothiazole) showed the lowest docking showed score of-5.903kcal/mol (Figure).

Fig. 18: Leptin (ID: 3V6O)

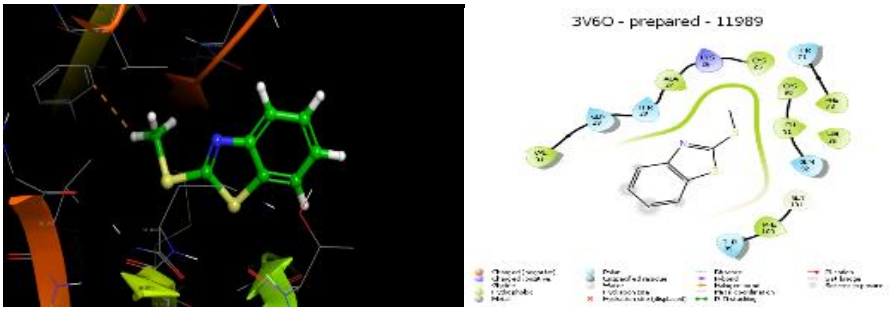

Fig. 19: Molecular interactions of leptin (ID: 3V6O)

The active site residues such as Pro-10, Thr-24, Thr-28, Cys-90, Thr-99, The-100, Ser-102, Gly-103, Thr-104 formed in molecular interactions were also well correlated with the active site residues of native Leptin (ID: 3V6O) and the Lys-11, cys-25, Lys-26, Ala-27, Thr-28, Gln-29, Val-31, Cys-19, Gln-92, Trp-94, Asn-95, Thr-96, Pro-97, Gly-101 were around the active site (within 4 A°) found to be present involed in van der Waals interactions with ligand.

Analysis of docking results revealed that ligand interaction Leptin (ID: 3V6O) docking complex showed good binding affinity, binding oreintation, pharmocological properties. The formation of hydrogen bond along with the residues involed in van der Waals interctions were also highly important for the stability of the docking complex. Hence, lead-1with better docking score (-5.903kcal/mol). Hence, the best ligands were proposed as the best antagonist to block Leptin (ID: 3V6O) of, which plays a major role in the drug development pathways.

Table 13: Docking score of leptin (ID: 3V6O) with ligands

S. No.	Title	Donor HB	Accpt HB	Glide rotatable bonds	Docking score
1	11989	0	1.5	1	-5.903
2	240	0	2	1	-5.013
3	129532628	2	9.1	4	-4.949
4	5281328	1	1.7	6	-4.78
5	8030	0	0	0	-4.527
6	69435	3	3.7	3	-4.515
7	72805	2	9.8	0	-4.292
8	123435	2	8.1	0	-4.171
9	5281239	1	7.45	14	-3.63
10	88095	0	7.9	6	-3.21
11	1032	1	2	1	-2.47
12	101922872	4	9.4	15	-1.328

*Hydrogen bond donor (<5), *Hydrogen bond acceptor (<10), *Number of rotatable bonds, *Docking score.

Table 14: H-bond donor and acceptor and rotatable bonds and docking score with leptin with ligands

S. No.	Title	Q Plog Po/w	QP log S	QPP Caco	QP log BB	QPP mdck	Q Plog Kp	Q Plog Khsa	Percent human oral absorption	Rule of five	Rule of three
1	11989	3.031	-2.735	6656.771	0.574	10000	-1.097	-0.074	100	0	0
2	240	1.479	-1.116	1830.242	-0.08	950.803	-2.121	-0.657	94	0	0
3	129532628	-0.047	-1.192	100.862	-0.959	53.808	-3.752	-1.126	62.533	0	0
4	5281328	7.522	-8.722	3405.278	-0.292	1860.133	-1.718	2.071	100	1	1
5	8030	1.815	-1.449	9906.038	0.192	10000	-0.841	-0.374	100	0	0
6	69435	-3.351	0.054	10.81	-0.639	5.218	-6.624	-1.026	25.826	0	1
7	72805	0.099	2	402.712	0.098	226.545	-4.275	-1.265	74.148	0	0
8	123435	-0.235	-0.015	286.124	1.068	156.57	-6.292	-0.528	69.536	0	0
9	5281239	9.739	-12.081	395.845	-2.829	181.686	-1.725	2.441	100	2	2
10	88095	-1.384	1.316	1124.064	-0.516	561.37	-2.972	-1.949	73.443	0	0
11	1032	0.606	0.284	239.776	-0.284	134.41	-3.405	-0.962	73.087	0	0

*Molecular weight (<500 Da), *Predicted octanol/water partition co-efficient log P (acceptable range-2-6.5), *Predicted aqueous solubility test: S Mol/l(acceptable range6.5-0.5), *Apparent $Caco_2$ permeability nm/sec(<25 poor and>500 high), *prediction of brain/blood; (acceptable range-3.0-1.2),*Predicted apparent MDCK cell permeability in nm/s (<25 poor and>500 high),*log Kp for skin permeability (Kp in cm/hr), *log Khas serum protein binding (-1.5-1.5), Lipinski rule of five violation (max is 4), Jorgenson rule of 3 violation (max is 3), *Percentage of Human oral absorption(<25%is poor and>80% is high ADMET PROPERTIES: absorption, distribution, metabolism, excretion, toxicity.

Orlistat with anti-obesity proteins

Around the active site residues, a 10Å x 10Å x 10Å receptor grid was created for anti-obesity proteins. Initial docking of orlistat with anti-obesity proteins docked with significant docking score. The best lead PPAR-γ (ID: 4CI5) showed the lowest docking showed score of-7.716 kcal/mol (Figure).

PPAR-γ (ID: 4CI5) with His-194, Ser-201, Arg-201, Asn213, Trp-303, Gln-442, forming 1 hydrogen bond, and His-305 forming 2 hydrogen bonds. Additionally, Arg-203 forms one Pi-cation interaction and two salt bridges, while Lys-237 forms one salt bridge. Moreover, His-305 forms one salt bridge, and Phe-446 forms a Pi-Pi interaction with the ligand, FTO (ID: 3LFM), with Lys-216 forming one hydrogen bond. Leptin (PDB ID: 3V6O) interacts with Trh-24 and Lys26,

forming two hydrogen bonds. However, Resistin (ID: 1RFX) shows no interactions.

Analysis of docking results revealed that ligand interaction Orlistat with PPAR-γ (ID: 4CI5), α-Glucosidase (ID: 7K9N), FTO (ID: 3LFM), Resistin (ID: 1RFX), Leptin (ID: 3V6O) docking complex showed good binding affinity, binding orientation, pharmocological properties. The formation of hydrogen bond along with the residues involved in van der Waals interactions were also highly important for the stability of the docking complex. Hence, the lead PPAR-γ (ID: 4CI5) with a better docking score (-7.716 kcal/mol). Hence, the Standard was proposed as the best antagonist to block aminoglycoside 6'-N-acetyltransferase (Aac(6')-lb), which plays a major role in the drug development pathways.

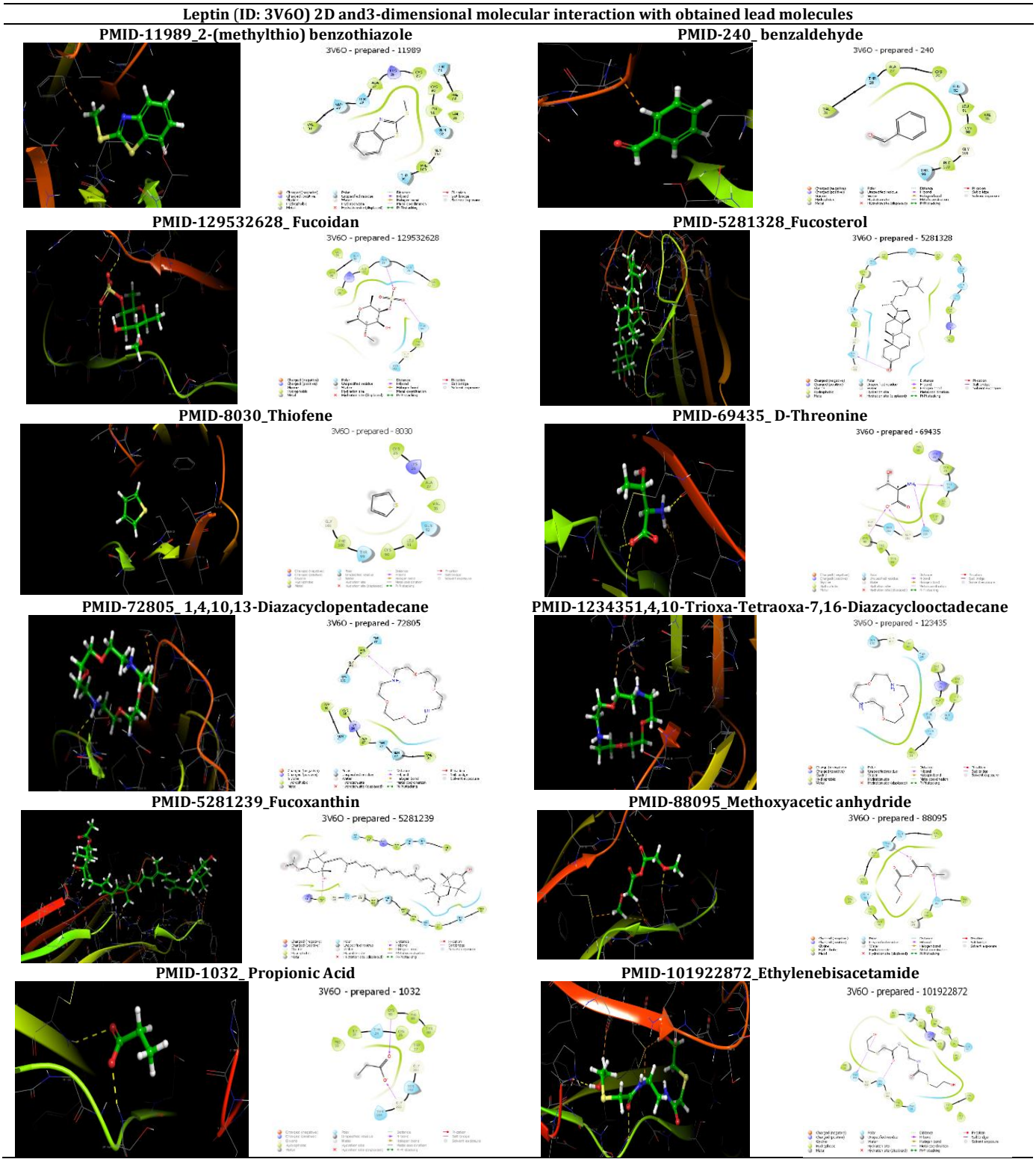

Fig. 20: Molecular interactions of leptin (PDB ID: 3V6O) with ligands

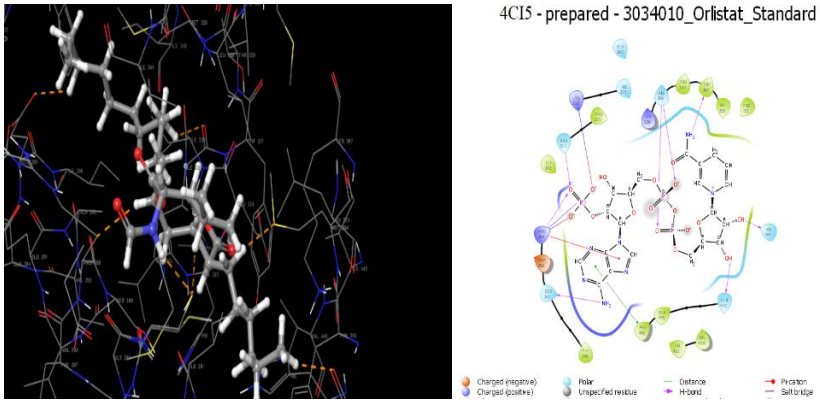

Fig. 21: Molecular interactions of orlistat with PPAR-γ (ID: 4CI5)

Table 15: ADMET properties of antioxidant and anti-obesity proteins with orlistat

Standard ligand	Protein name	Mol MW	Q Plog Po/w	Q Plog S	QPP Caco	Q Plog BB	QPP MDCK	Q Plog Kp	Q Plog Khsa	Percent Human oral absorption	Rule of five	Rule of three
3034010_ Orlistat_ Standard	4CI5 7K9N 3LFM 1RFX 3V6O	495.741	6.096	-7.182	153.403	-2.868	131.94	-2.375	0.845	88.803	1	1

*Molecular weight (<500 Da), *Predicted octanol/water partition coefficient log P (acceptable range-2-6.5), *Predicted aqueous solubility test: S Mol/l(acceptable range6.5-0.5), *Apparent $Caco_2$ permeability nm/sec(<25 poor and>500 high), *prediction of brain/blood; (acceptable range-3.0-1.2),*Predicted apparent MDCK cell permeability in nm/s (<25 poor and>500 high),*log Kp for skin permeability (Kp in cm/hr), *log Khsa serum protein binding (-1.5-1.5), Lipinski rule of five violation (max is 4), Jorgenson rule of 3 violation (max is 3), *Percentage of Human oral absorption (<25%is poor and>80% is high), ADMET properties.

Table 16: Docking score of orlistat with anti-obesity genes

Protein name	Docking score
4CI5	-7.716
1LFM	-2.661
3V6O	-4.419
7K9N	-2.801

*Hydrogen bond donor (<5), * Hydrogen bond acceptor (<10), *Number of rotatable bonds*

a) Interactions of Orlistat with antioxidant and anti-obesity genes

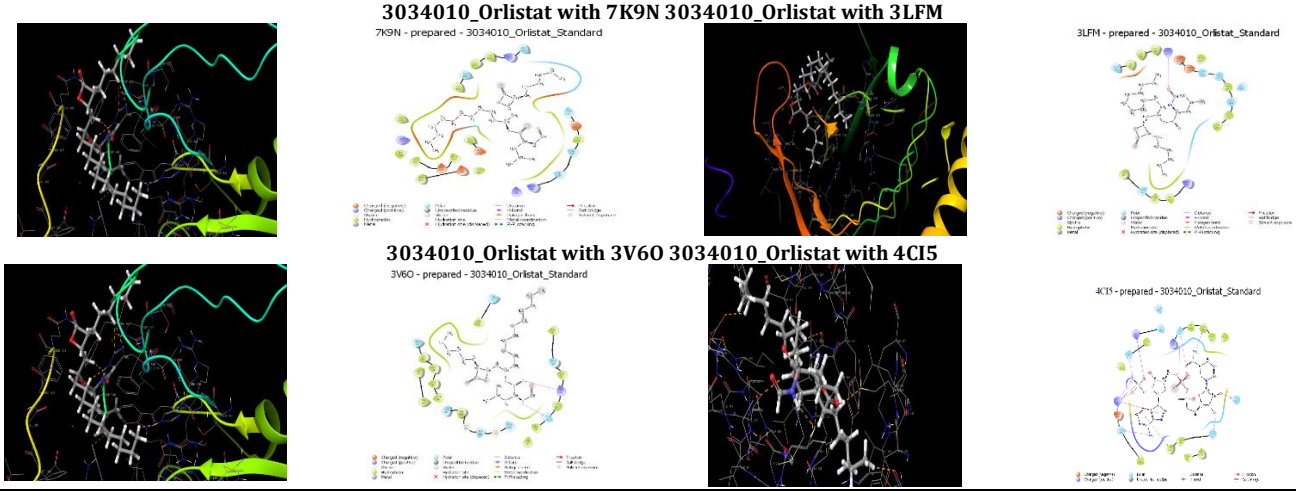

Fig. 22: Molecular interactions of orlistat with anti-obesity genes

DISCUSSION

Natural compounds play a pivotal role in therapeutic applications due to negligible adverse effects. Therefore, scientific knowledge towards acute oral toxicity study is much needed, which will not only help identify the range and concentration of dose that could be used subsequently but also to reveal the possible clinical signs elicited by the substances under investigation. In UPEE and MOME

have good bio active compounds. The result was compared with reference anti-obesity drug, orlistat. Strong binding affinities are shown by the study's results with important targets related to obesity, such as PPAR-γ (ID: 4CI5), (ID: 3LFM), Resistin (ID: 1RFX), Leptin (ID: 3V6O) as well as with the UPEE and MOME.

Carboxyl, sulfhydryl, and OH functional groups the primary seaweed constituents and those derived from polysaccharides are involved in the uptake of seaweed [23]. UPEE has numerous bioactive properties such as antioxidant and anticancer activities [24]. Fucoidan isolated from brown seaweeds UPEE showed interesting antitumor activity due to its various biological activities [25]. Brown algae *Barbus barbus* as a natural source of bioactive substances (chlorophylls and carotenoids) [26]. In present study, Fourier infrared spectroscopy examination of UPEE revealed the presence of phenols, OH groups, phenols, carboxylic acids, halogens, methyl groups vinyl compounds, amides, alkenes, and alkyl halide organic compound groups. Fourier infrared spectroscopy examination of in herbal medicine analysis [27]. Main structure of herbal materials adds the complexity of FTIR spectra interpretation. About the spectral behaviour of homogenized herbal and herbal extracts [28]. MOME revealed the presence of phenols, aldehyde alkanes, amines, methyl groups vinyl compounds, amides, OH groups and carboxylic acids organic compound groups.

GC-MS analysis of *Undaria pinnatifida* revealed the presence of bioactive compounds such as fucosterol, 1,3, Difluro-2-propanol, benzaldehyde, hexaborane and 2-(3-Methylphenoxy) octahydro-1H-1,3,2-benzodiazaphosphole 2-oxide the important medicinal properties. Glycoprotein isolated from UPEE and tested for antioxidant activities using an *in vitro* digestion model [29, 30]. GC-MS analysis of cinnamon bark indicated the presence of *trans*-cinnamaldehyde [31]. Hence, the presence of these compounds was responsible for the therapeutic effects. The phytochemical and GC-MS profiling of *moringa oleifera* revealed the presence of bioactive compounds such as pentaborane, D-Threonine,13-pentano-1,4,10-trioxa-7,13-diazacyclopentadecane, propanoic acid and hydroxy propanoic acid with important medicinal properties. Hence, the presence of these phytochemicals could be responsible for the therapeutic effects.

1,4,10-Trioxa-7,13-diazacyclopentadecane_1234352-methylthio)benzothiazole, benzaldehyde, di methyl pentathiophene, D-threonine, fucoxanthin, fucosterol, fucoidan, thiophene, hexaborane, methoxyacetic_anhydride, NN ethylene bis acetamide,1,4,10,13-tetraoxa-7,16-diazacyclooctadecane ligands were docked anti-obesity proteins among all 13 ligands PPAR-γ (PDB ID: 4CI5) with fucosterol (-6.709kcal/mol), α-glucosidase (PDB ID: 7K9N) with trioxadiazacyclopentadecane (-6.466kcal/mol), FTO, (PDB ID: 3LFM)with bbenzothiazole (-5.566kcal/mol), Resistin(PDB ID: 1RFX) with benzothiazole (-5.322kcal/mol), leptin (PDB ID: 3V6O) with 2-methylthio benzothiazole (-5.903 kcal/mol) showed best docking score.

The docking findings analysis showed that the interaction of the ligand Orlistat standard with the PPAR-γ (ID: 4CI5), α-Glucosidase (ID: 7K9N), FTO (ID: 3LFM), Resistin(ID: 1RFX), Leptin(ID: 3V6O)demonstrated good binding affinity, binding organisation, and pharmacological characteristics. For the docking complex to remain stable, hydrogen bond formation and residues involved in van der Waals interactions were both crucial. Lead PPAR-γ has the best docking score (-7.716 kcal/mol), as a result. As a result, the standard was recommended as the best antagonist to block the key enzyme involved in the drug development pathways, aminoglycoside 6'-N-acetyltransferase (Aac(6')-Ib).

CONCLUSION

In this study, we investigated the anti-obesity potential of bioactive components from MOME and UPEE using *in silico* methodologies. Using molecular docking investigations and virtual screening, we found intriguing drugs that have robust interactions with important targets related to obesity, such as PPAR-γ (ID: 4CI5), Leptin (ID: 3V6O) and FTO (ID: 3LFM). These results point to the possibility of additional experimental validation. Although computational approaches provide insightful information, they are only the first stage in the drug discovery process. Bioactivity, toxicology, and pharmacokinetic assays are only a few of the rigorous experiments needed to determine these drugs' genuine therapeutic value. The benefits of combining traditional knowledge with computational methods highlight the value of multidisciplinary study. The potential of UPEE and MOME as sources of bioactive chemicals that combat obesity is highlighted by this research, which aids in the hunt for novel therapeutic agents. Translating these findings into workable remedies to the obesity pandemic will require cooperation among experts in different domains.

FUNDING

Nil

AUTHORS CONTRIBUTIONS

All authors have contributed equally

CONFLICT OF INTERESTS

Declared none

REFERENCES

1. Qasim A, Turcotte M, de Souza RJ, Samaan MC, Champredon D, Dushoff J. On the origin of obesity: identifying the biological, environmental and cultural drivers of genetic risk among human populations. Obes Rev. 2018 Feb;19(2):121-49. doi: 10.1111/obr.12625, PMID 29144594.
2. Saunders KH, Igel LI, Shukla AP, Aronne LJ. Drug-induced weight gain: rethinking our choices. J Fam Pract. 2016 Nov;65(11):780-8. PMID 28087864.
3. Bastien M, Poirier P, Lemieux I, Despres JP. Overview of epidemiology and contribution of obesity to cardiovascular disease. Prog Cardiovasc Dis. 2014 Jan-Feb;56(4):369-81. doi: 10.1016/j.pcad.2013.10.016, PMID 24438728.
4. Birari RB, Bhutani KK. Pancreatic lipase inhibitors from natural sources: unexplored potential. Drug Discov Today. 2007 Oct;12(19-20):879-89. doi: 10.1016/j.drudis.2007.07.024, PMID 17933690.
5. Moreno Cordova EN, Arvizu Flores AA, Valenzuela Soto EM, Garcia Orozco KD, Wall Medrano A, Alvarez Parrilla E. Gallotannins are uncompetitive inhibitors of pancreatic lipase activity. Biophys Chem. 2020 Sep;264:106409. doi: 10.1016/j.bpc.2020.106409, PMID 32534374.
6. Chaput JP, Berube Parent S, Tremblay A. Obesity and cardiovascular physiology: impact of some pharmacological agents. Curr Vasc Pharmacol. 2005 Apr;3(2):185-93. doi: 10.2174/1570161053586886, PMID 15853638.
7. Cheung BM, Cheung TT, Samaranayake NR. Safety of antiobesity drugs. Ther Adv Drug Saf. 2013 Aug;4(4):171-81. doi: 10.1177/2042098613489721, PMID 25114779, PMCID PMC4125319.
8. Grasa Lopez A, Miliar Garcia A, Quevedo Corona L, Paniagua Castro N, Escalona Cardoso G, Reyes Maldonado E. Undaria pinnatifida and fucoxanthin ameliorate lipogenesis and markers of both inflammation and cardiovascular dysfunction in an animal model of diet-induced obesity. Mar Drugs. 2016 Aug 3;14(8):148. doi: 10.3390/md14080148, PMID 27527189, PMCID PMC4999909.
9. Sofowora A. Recent trends in research into African medicinal plants. J Ethnopharmacol. 1993 Mar;38(2-3):209-14. doi: 10.1016/0378-8741(93)90017-y, PMID 8510470.
10. Jiang S, Yu M, Wang Y, Yin W, Jiang P, Qiu B. Traditional cooking methods affect color, texture and bioactive nutrients of *Undaria pinnatifida*. Foods. 2022;11(8):1078. doi: 10.3390/foods11081078, PMID 35454666.
11. Ali Redha AA, Perna S, Riva A, Petrangolini G, Peroni G, Nichetti M. Novel insights on the anti-obesity potential of the miracle tree, moringa oleifera: a systematic review. J Funct Foods. 2021;84:104600. doi: 10.1016/j.jff.2021.104600.
12. Kim DS, Choi MH, Shin HJ. Extracts of moringa oleifera leaves from different cultivation regions show both antioxidant and antiobesity activities. J Food Biochem. 2020 Jul;44(7):e13282. doi: 10.1111/jfbc.13282, PMID 32436270.

13. Daghaghele S, Kiasat AR, Safieddin Ardebili SM, Mirzajani R. Intensification of extraction of antioxidant compounds from *Moringa Oleifera* leaves using the ultrasound-assisted approach: BBD-RSM design. International Journal of Fruit Science. 2021;21(1):693–705. doi: 10.1080/15538362.2021.1926396
14. Bhattacharya A, Tiwari P, Sahu PK, Kumar S. A review of the phytochemical and pharmacological characteristics of *Moringa oleifera*. J Pharm Bioallied Sci. 2018 Oct-Dec;10(4):181-91. doi: 10.4103/JPBS.JPBS_126_18, PMID 30568375, PMCID PMC6266645.
15. Avwioroko OJ, Anigboro AA, Otuechere CA, Atanu FO, Dairo OF, Oyetunde TT. α-amylase inhibition, anti-glycation property and characterization of the binding interaction of citric acid with α-amylase using multiple spectroscopic, kinetics and molecular docking approaches. J Mol Liq. 2022;360:119454. doi: 10.1016/j.molliq.2022.119454.
16. Moreno Cordova EN, Arvizu Flores AA, Valenzuela Soto EM, Garcia Orozco KD, Wall Medrano A, Alvarez Parrilla E. Gallotannins are uncompetitive inhibitors of pancreatic lipase activity. Biophys Chem. 2020;264:106409. doi: 10.1016/j.bpc.2020.106409, PMID 32534374.
17. Alasalvar C, Ozturk N, Gokce H, Guder A, Mentese E, Bektaş H. Synthesis, structural, spectral, antioxidant, bioactivity and molecular docking investigations of a novel triazole derivative. J Biomol Struct Dyn. 2022;40(14):6642-55. doi: 10.1080/07391102.2021.1887764, PMID 33594957.
18. McNaught AD. Compendium of chemical terminology. Vol. 1669. Oxford: Blackwell Publishing Science; 1997.
19. Dandekar R, Fegade B, Bhaskar VH. GC-MS analysis of phytoconstituents in alcohol extract of epiphyllum oxypetalum leaves. J Pharmacogn Phytochem. 2015;4(1):148-54.
20. Rester U. From virtuality to reality-virtual screening in lead discovery and lead optimization: a medicinal chemistry perspective. Curr Opin Drug Discov Devel. 2008 Jul;11(4):559-68. PMID 18600572.
21. Rollinger JM, Steindl TM, Schuster D, Kirchmair J, Anrain K, Ellmerer EP. Structure-based virtual screening for the discovery of natural inhibitors for human rhinovirus coat protein. J Med Chem. 2008;51(4):842-51. doi: 10.1021/jm701494b, PMID 18247552.
22. Ballester PJ, Mitchell JBO. A machine learning approach to predicting protein-ligand binding affinity with applications to molecular docking. Bioinformatics. 2010;26(9, May):1169-75. doi: 10.1093/bioinformatics/btq112, PMID 20236947.
23. Dzobo K. The role of natural products as sources of therapeutic agents for innovative drug discovery. Compr Pharmacol. 2022:408-22. doi: 10.1016/B978-0-12-820472-6.00041-4, PMCID PMC8016209.
24. Kannan S. FT-IR and EDS analysis of the seaweeds sargassum wightii (brown algae) and gracilariacorticata (red algae). Int J Curr Microbiol Appl Sci. 2014;3(4):341-51.

s

25. Koh HSA, Lu J, Zhou W. Structure characterization and antioxidant activity of fucoidan isolated from Undaria pinnatifida grown in New Zealand, carbohydrate Polymers. 2019;212:178-85. doi: 10.1016/j. carbpol.2019.02.040.
26. Synytsya A, Kim WJ, Kim SM, Pohl R, Alla Synytsya F. Kvasnicka, Jana Copikova, Yong Il Park, Structure and antitumour activity of fucoidan isolated from sporophyll of Korean brown seaweed Undaria pinnatifida, carbohydrate. Polymers. 2010;81(1):41-8. doi: 10.1016/j.carbpol.2010.01.052.
27. Hentati F, Barkallah M, Ben Atitallah A, Dammak M, Louati I, Pierre G. Quality characteristics and functional and antioxidant capacities of algae-fortified fish burgers prepared from common barbel (Barbus barbus). BioMed Res Int. 2019. doi: 10.1155/2019/2907542, PMID 31687385.
28. Bunaciu AA, Aboul-Enein HY, Fleschin S. Recent applications of fourier transform infrared spectrophotometry in herbal medicine analysis. Appl Spectrosc Rev. 2011;46(4):251-60. doi: 10.1080/05704928.2011.565532.
29. Brangule A, Sukele R, Bandere D. Herbal medicine characterization perspectives using advanced FTIR sample techniques-diffuse reflectance (DRIFT) and photoacoustic spectroscopy (PAS). Front Plant Sci. 2020;11:356. doi: 10.3389/fpls.2020.00356, PMID 32362902.
30. Barth A. Infrared spectroscopy of proteins. Biochim Biophys Acta. 2007;1767(9):1073-101. doi: 10.1016/j.bbabio.2007.06.004, PMID 17692815.
31. Rafiquzzaman SM, Kim EY, Kim YR, Nam TJ, Kong IS. Antioxidant activity of glycoprotein purified from Undaria pinnatifida measured by an *in vitro* digestion model. Int J Biol Macromol. 2013;62:265-72. doi: 10.1016/j.ijbiomac.2013.09.009, PMID 24060280.
32. Li YQ, Kong DX, Wu H. Analysis and evaluation of essential oil components of cinnamon barks using GC–MS and FTIR spectroscopy. Ind Crops Prod. 2013;41:269-78. doi: 10.1016/j.indcrop.2012.04.056.
33. Katelia R, Jauhar MM, Syaifie PH, Nugroho DW, Ramadhan D, Arda AG. In silico investigation of xanthone derivative potency in inhibiting carbonic anhydrase II (ca ii) using molecular docking and molecular dynamics (md) simulation. Int J App Pharm. 2022;14(5):190-8. doi: 10.22159/ijap.2022v14i5.45388.
34. Muhaimin M, Chaerunisaa AY, Rostinawati T, Amalia E, Hazrina A, Nurhasanah S. A reviewon nanoparticles of Moringa oleifera extract: preparation, characterization, and activity. Int J App Pharm. 2023;15(4):43-51. doi: 10.22159/ijap.2023v15i4.47709.
35. Bhange A, Pethe A, Hadke A. Design and development of phytosomal soft nanoparticles for liver targeting. Int J App Pharm. 2023;15(1):280-9. doi: 10.22159/ijap.2023v15i1.46303.
36. SR, RV, PA. GCMS analysis on andrographis paniculata seed extract and its anticancer activity. International Journal of Applied Pharmaceutics. 2022;14:84-88. doi: 10.22159/ijap.2022.v14ti.5.